Studies in Transition and Time Varying Turbulent Flows

Final Report

Principal Investigator - Chester E. Grosch

12 November 2003 to 11 February 2004

Old Dominion University, Norfolk, Virginia 23529

Grant NAG1-1-02005

Abstract

The reasearch focused on two areas; (a) the dynamics of forced turbulent flows and (b) time filtered Large Eddy Simulations (TLES). The dynamics of turbulent flows arising from external forcing of the turbulence are poorly understood. In particular, here are many unanswered questions relating the basic dynamical balances and the existence or nonexistence of statistical equilibrium of forced turbulent flows. This research used direct numerical simulations to explore these questions. The properties of the temporally filtered Navier-Stokes equations were also studied

Forced Isotropic Turbulence

The physics of turbulent flows arising from time varying mean flow or forcing is very complex. There is no accepted theory which can be applied to these types of flows. Experiments on these types of flows are problematical because of the uncertainty in what is statistical equilibrium and whether or not such a state exists or can exist for these classes of flows. Thus there is a lack of understanding as to which quantities should be measured and interpreted.

Direct numerical simulation (DNS) is a well known technique for studying the dynamics of turbulent flows at low and moderate Reynolds numbers. In a pioneering study Rogallo[1] carried out a DNS of decaying isotropic turbulence. This flow is in a statistical equilibrium at each instant of time, albeit that the statistical moments, spectrum, etc. are slowly varying functions of time.

here we consider both decaying isotropic turbulence and isotropic turbulence with forcing. The forcing in the present study was applied to a DNS of a turbulent flow in statistical equilibrium. The DNS code is pseudo-spectral in two directions (x_1, x_3) and uses fourth order finite differences in the other (x_2) direction. The time advancement is done by using a third-order, low storage Runge-Kutta method. The boundary conditions are periodic in all directions in a cube of size L. The effect of the forcing must depend on the "size" of the forcing function relative to the "size" of the turbulent structures. To be more precise, consider the spectrum of, say, isotropic turbulence. In statistical equilibrium the shape of the spectrum is invariant and contains (1) an energy containing range, (2) an energy transfer range wherein the energy from the energy containing range is transferred to (3) the energy dissipation range. These three ranges have different "size" turbulent structures with the "size" decreasing from (1) thru (2) to (3). Therefore the effect of forcing will depend on in which range the "size" of the forcing function matches the "size" of the turbulent structures.

The most natural way to match the "size" of the forcing function to the "size" of the turbulent structures is to do so in wavenumber (Fourier) space rather than physical space. This arises because, in wavenumber space, the "size" of the turbulent structure is precisely defined by the inverse of the corresponding wavenumber. Thus the forcing was done in wavenumber space and was applied in each of the three significant dynamical ranges: the energy containing range, the energy transfer range and the energy dissipation range. These correspond, in wavenumber space, to the small wavenumbers, the intermediate wavenumbers and the large wavenumbers.

In applying the forcing the objective is fix the energy in the particular range chosen while permitting these Fourier modes to interact with themselves and all of the other modes. To see how this can be done, one notes that the energy of a particular Fourier mode is proportional to the absolute value of the complex Fourier amplitude of that mode while mode-mode interactions are essentially controlled by phase interactions. Thus to fix the energy in the particular range of wavenumbers the *amplitudes* of the Fourier modes in this range must be held fixed and to permit these Fourier modes to interact with themselves and all of the other modes requires that the *phases* of these Fourier modes be allowed to evolve in accordance with the underlying dynamics, that is, be governed by the Navier-Stokes equations.

An algorithm to accomplish this requires an initialization and implementation at each time step. The initialization consists of first choosing a range of wave numbers, second Fourier analyzing the velocity field and third, storing the amplitude of every Fourier mode in the appropriate range, perhaps after having multiplied each of them by some wavenumber forcing function. Then, at every subsequent time step, the velocity field must be Fourier analyzed and the amplitude of the Fourier modes in the forcing range be set equal to the stored amplitude while retaining the phase unchanged. Finally, this field is inverse Fourier transformed to produce a velocity field with the prescribed forcing amplitude and appropriate phase distribution. No changes need be made to the pressure field because it is calculated using the gradients of the velocity field and so will be consistent with the velocity field.

The results of these DNSs are being analyzed in terms standard dynamical quantities, energy, dissipation rate, two-point correlations, spectra and so on, in order to determine the effects of forcing in each of these ranges. Some preliminary results for the case of forcing at high wavenumbers, $30 \leq k \leq 32$, are presented here.

Results of Forcing the High Wavenumbers of Isotropic Turbulence

Figure 1 is a plot of energy spectra, E(k), as a function of the wavenumber, k. The dashed black curve is the spectrum at time t_o at which forcing began. The colored dashed curves are the spectra of the unforced turbulence and the colored solid curves are the spectra of the forced turbulence at the same time as the unforced turbulence. These results are for three succeding times: red is at t_1 ($t_1 > t_o$), green is at t_2 ($t_2 > t_1$) and green is at t_3 ($t_3 > t_2$). The solid black line has a slope of $-5/3$. Comparision of the dashed curves shows that the unforced turbulence has reached a self-similar state and that the energy is decaying in time. On the other hand, the forced turbulence shows different behavior at high wavenumbers as compared to low wavenumbers. At low wave numbers, say $k \leq 20$, the decaying turbulence is self-similar. The forced peak in $30 \leq k \leq 32$ is unchanged in time. There is a small region in wavenumber space, $20 \leq k \leq 30$ where "back scatter", *i.e.* energy transfered from higher to lower wavenumber is apparent. Finally, for $k > 32$, the energy level of the forced turbulence, while decaying in time, is, at any time, higher than that of the unforced turbulence because of the transfer of energy from the band of wavenumbers where the forcing is occuring.

The dissipation spectra are plotted in Figure 2 with the same conventions of dashed, solid and color as in Figure 1. The peak in the dissipation spectra of the unforced turbulence shifts to lower wavenumber as time increases; it is at k about 18 at t_o and at k about equal to 12 at t_3. The forced turbulence shows similar behavior but this is a secondary peak with the main peak being that in the forcing wavenumber range and this peak remains constant in time. The "back scatter" is also readily apparent in this figure.

The isotropy of the turbulence is most readily checked by examining the correlation functions, here correlations in space at fixed times. The longitudinal and transverse correlations for the unforced turbulence at t_3 are shown in Figure 3. The notation in this figure is of the form $\rho_{i,i}(x_j)$ and this denotes the autocorrelation of velocity component u_i at spatial separation x_j with the index k being the value of $x_j/\Delta x_j$. The top panel in Figure 3 shows the longitudinal autocorrelation functions of u_1 in the x_1 direction (solid), u_2 in the x_2 direction (dash) and u_3 in the x_3 direction (dash-dot). The three longitudinal autocorrelation functions are essentially equal with only minor differences at large k (large separation). These autocorrelation functions decay to zero at about k = 30. The middle panel shows the first of the transverse autocorrelation functions, that of u_1 in the x_2 direction (solid), u_2 in the x_3 direction (dash) and u_3 in the x_1 direction (dash-dot). These functions are essentially equal for k $\leq$ 10 and have minor differences at larger wavenumbers. Finally, the bottom panel in Figure 3 shows the second set of transverse autocorrelation functions, that of u_1 in the x_3 direction (solid). u_2 in the x_1 direction (dash) and u_3 in the x_2 direction (dash-dot). These functions are very similar to the first set of transverse autocorrelation functions. The longitudinal integral length scale. $L_l = 10.367$ and the two transverse integral length scales, $L_{tj} = 4.997$ and 4.996 for $j = 1.2$ and the ratio. $L_l/L_{tj} = 2.075$. The behavior of these autocorrelation functions is those of isotropic turbulence. in particular having $L_{t1} = L_{t2}$ and L_l/L_{tj} approximately equal to 2 (Pope, 2001) The corresponding longitudinal and transverse correlations for the forced turbulence, also at t_3, are shown in Figure 4. The notation is the same as in Figure 3. Comparing Figures 3 and 4, there is no readily apparent difference and it appears that the forcing has little or no effect of these autocorrelation functions. There are, however. very small differences caused by the forcing at high wavenumber. These show up in the integral length scales. For this case of high wavenumber forcing of isotropic turbulence the longitudinal integral length scale. $L_l = 10.014$ and the two transverse integral length scales. $L_{tj} = 4.831$ and 4.822 for $j = 1, 2$ and the ratio, $L_l/L_{tj} = 2.073$ and 2.077 for $j = 1.2$. The high wavenumber forcing increases the relative amount of energy in the high wavenumbers as compared to the low wavenumbers. This has the effect of slightly reducing both the longitudinal integral length scale and both the transverse integral length scales as compared to the unforced flow. The ratios of these scales. however, remains quite close to 2 and they differ only in the fourth significant figure.

Figure 5 shows the spatial cross-correlations as functions of spatial separation. In this figure the solid curve corresponds to separation in the x_1 direction, the dash curve to separation in the x_2 direction and the dash-dot curve to separation in the x_3 direction. As in the previous figures the index $k = x_i/\Delta x_i$. As expected, these cross-correlations are quite small, with the absolute value of the maximum being approximately 0.05. Also, these cross-correlations show no symmetry about $k = 0$. The spatial cross-correlations for the forced case are shown in Figure 6. Comparing the results shown in these two figures one can note slight differences between the forced and unforced cases. These differences are most apparent near $k = 0$, roughly in the range $-5 \leq k \leq 5$. The high wavenumber forcing causes all of the cross-correlations to be equal in this range of k; again a subtle change in the structure of the turbulence caused by the forcing.

The next six figures. Figures 7 thru 12, show instantaneous contours of the velocity components, u_i. $i = 1, 2, 3$. on the plane $x_1 = 1/2$ at time t_3. Figures 7. 9 and 11 are for the unforced case and Figures 8, 10 and 12 are the results of the forced case. In Figure 7 the contours of u_1 for the unforced turbulence show structures whose sizes range from x_i/L about 0.05 to about 0.3. The area of positive u_1 (the red areas) is somewhat larger than the area of negative u_1 (the blue areas) but the maximum negative velocity is twice the maximum positive velocity. Figure 8 shows the contours of u_1 for the forced turbulence on the same plane and at the same time. Comparing these two figures one sees that the range of u_1 is unchanged and that the larger structures are the same in both figures. What is different is that forcing at the high wavenumbers has caused a much finer scale of motion within and between the larger scales. Figures 9 and 10 show contours of u_2 and Figures 11 and 12 show contours of u_3 on the same plane. These pairs of figures show that the forcing at high wavenumber have the same effect on u_2 and u_3 as on u_1.

Summary

Forcing isotropic tirbulence at high wave numbers has significant effects on both the energy and dissipation spectra: comparision of the energy spectra showed that the unforced isotropic turbulence had reached a self-similar state and that the energy was decaying in time. On the other hand, the forced iostropic turbulence showed a different behavior at high wavenumbers as compared to low wavenumbers. At low wave numbers, say $k \leq 20$, the decaying turbulence was self-similar. The forced peak in $30 \leq k \leq 32$ was unchanged in time. There was a small region in wavenumber space, $20 \leq k \leq 30$ where "back scatter" was apparent. Finally, for $k > 32$, the energy level of the forced isotropic turbulence, while decaying in time, was, at any time, higher than that of the unforced turbulence because of the transfer of energy from the band of wavenumbers where the forcing was occuring. The peak in the dissipation spectra of the unforced isotropic turbulence shifted to lower wavenumber as time increased, it was at k about 18 at t_o and at k about equal to 12 at t_3 and the forced turbulence showed similar behavior but this was a secondary peak with the main peak being that in the forcing wavenumber range and this peak remained constant in time with the "back scatter" also readily apparent.

The behavior of the longitudinal and transverse autocorrelation functions was shown to be that of isotropic turbulence, in particular having $L_{t1} = L_{t2}$ and L_l/L_{tj} approximately equal to 2 for both unforced and forced isotropic turbulence. There was no readily apparent difference between the two cases and it appeared that the forcing had little or no effect of the autocorrelation functions. There were, however, very small differences caused by the forcing at high wavenumber. These showed up in the integral length scales. The high wavenumber forcing increased the relative amount of energy in the high wavenumbers as compared to the low wavenumbers. This had the effect of slightly reducing both the longitudinal integral length scale and both the transverse integral length scales for the forced flow as compared to the unforced flow. The ratios of these scales, however, remained quite close to 2 and they differed only in the fourth significant figure. There are slight differences in the cross-correlations between the forced and unforced cases. These differences were most apparent near $k = 0$, roughly in the range $-5 \leq k \leq 5$. The high wavenumber forcing caused all of the cross-correlations to be equal in this range of k; again a subtle change in the structure of the isotropic turbulence caused by the forcing.

Comparing the velocity fields, $u_i, i = 1, 2, 3$ on the plane $x_1 = 1/2$ for the unforced and forced cases showed that the range of the of u_i was unchanged and that the larger structures are the same in both cases. What was different was that forcing at the high wavenumbers had caused a much finer scale of motion within and between the larger scales.

References

1. *Pope, S. B.*, "Turbulent Flows", *Cambridge University Press, Cambridge and New York. 2001.*

2. *Rogallo, R. S.*, "Numerical experiments in homogeneous turbulence", *NASA Technical Report TM81315, 1981.*

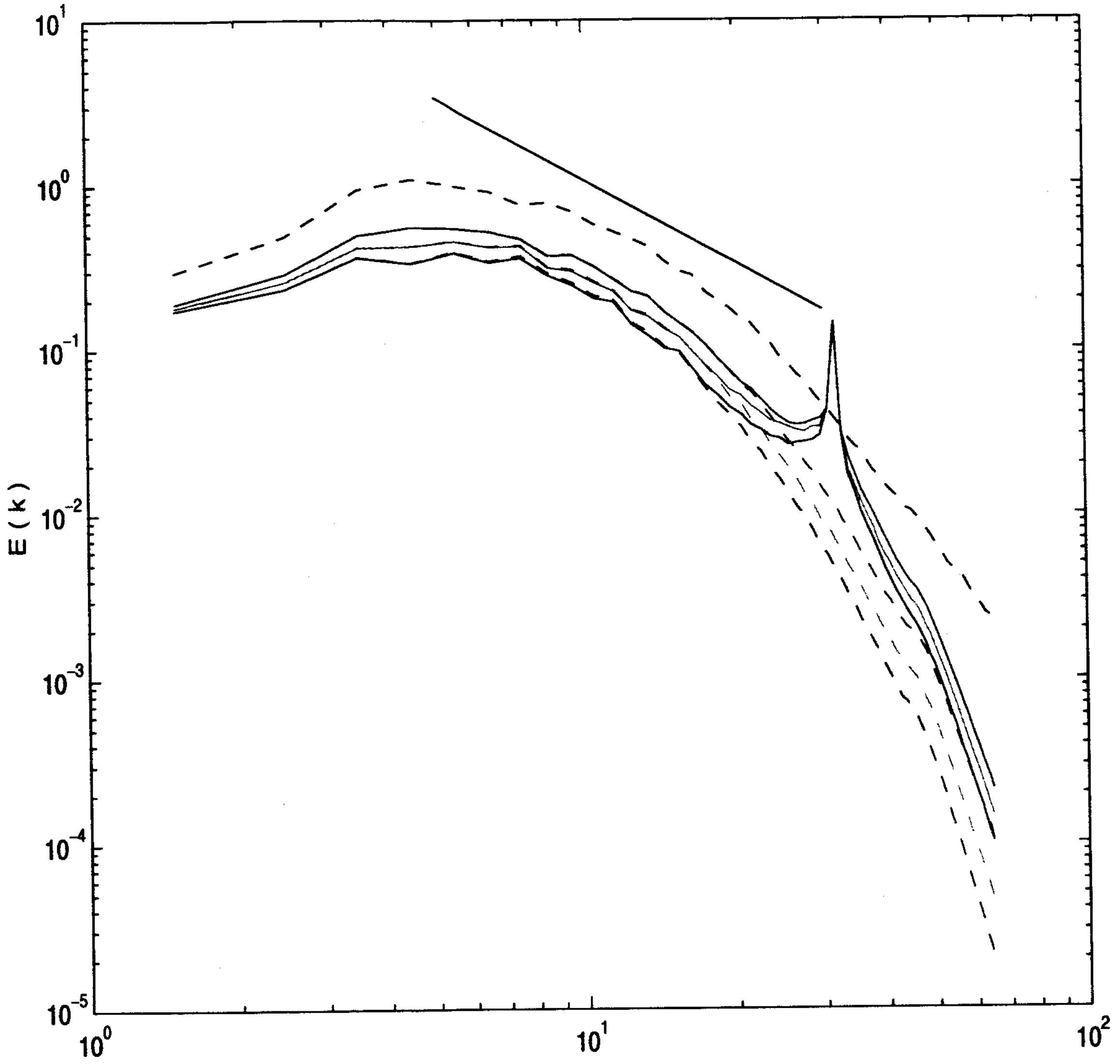

Figure 1: Energy spectra, E(k), as a function of the wavenumber, k. The dashed black curve is the spectrum at time t_o at which forcing began. The colored dashed curves are the spectra of the unforced turbulence and the colored solid curves are the spectra of the forced turbulence at the same time as the unforced turbulence. These results are for three succeding times; red is at t_1 ($t_1 > t_o$), green is at t_2 ($t_2 > t_1$) and blue is at t_3 ($t_3 > t_2$). The solid black line has a slope of $-5/3$.

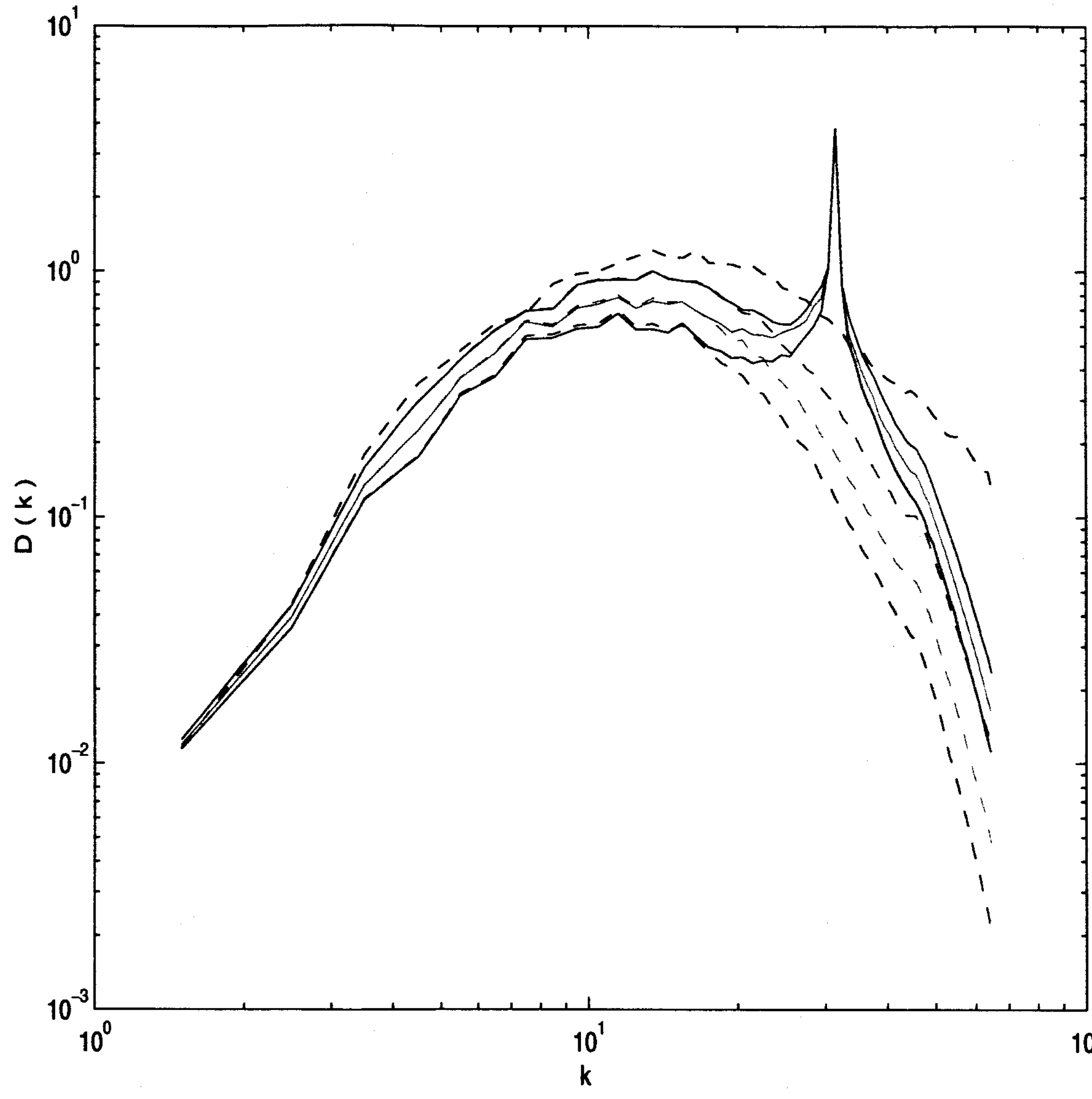

Figure 2: Dissipation spectra with the same conventions for the dashed and solid curves and for the colors as in Figure 1.

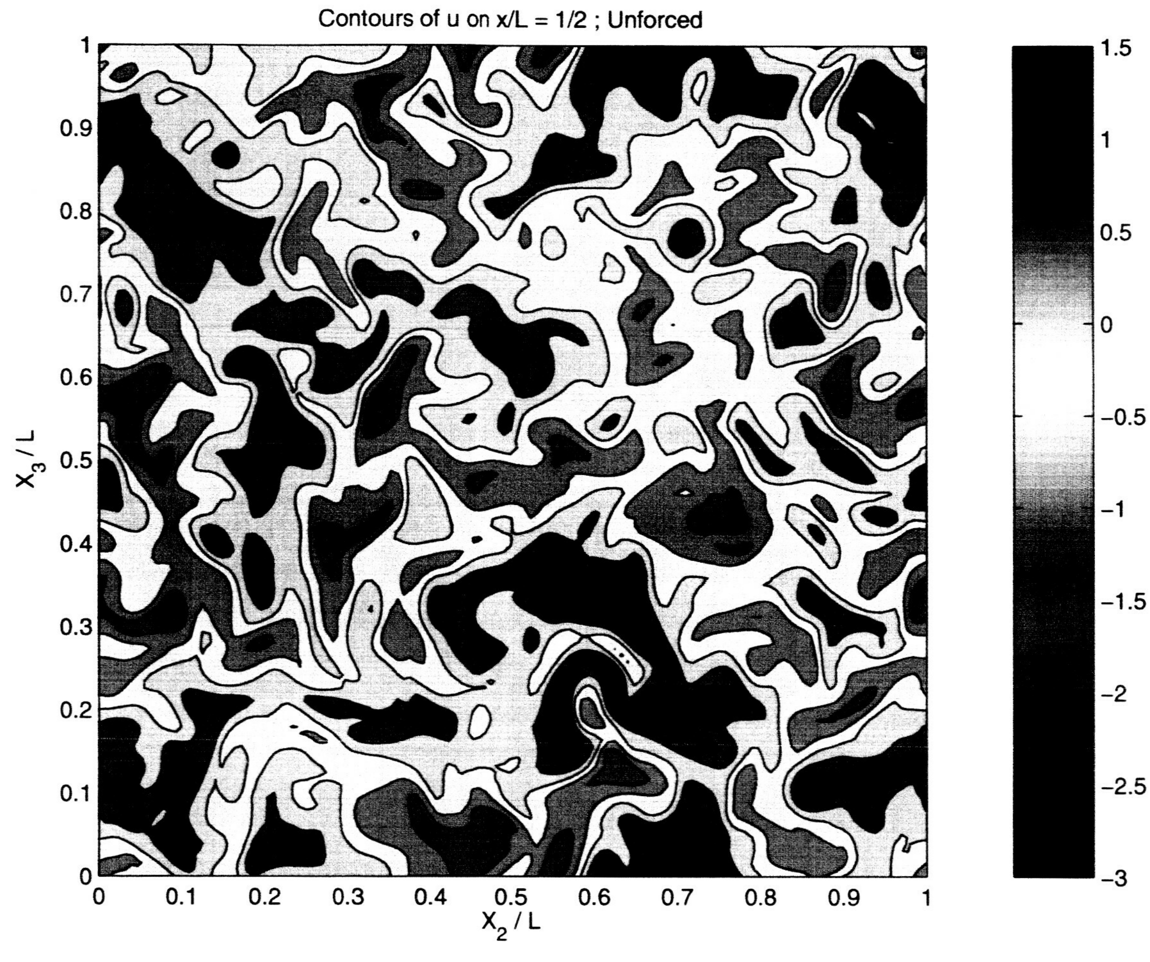

Figure 7: Contours of u_1 on the plane $x_1 = 1/2$ at time t_3 for the unforced flow.

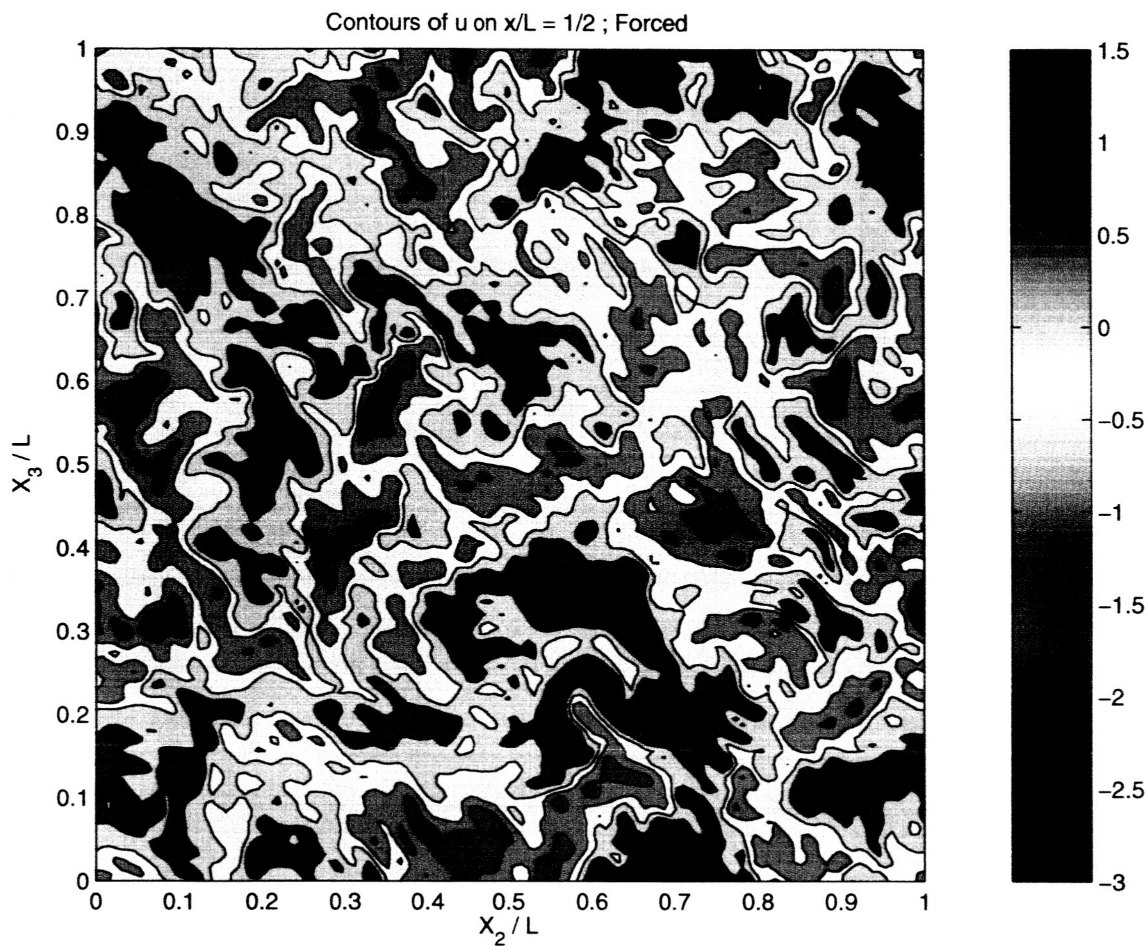

Figure 8: Contours of u_1 on the plane $x_1 = 1/2$ at time t_3 with forcing at high wavenumbers.

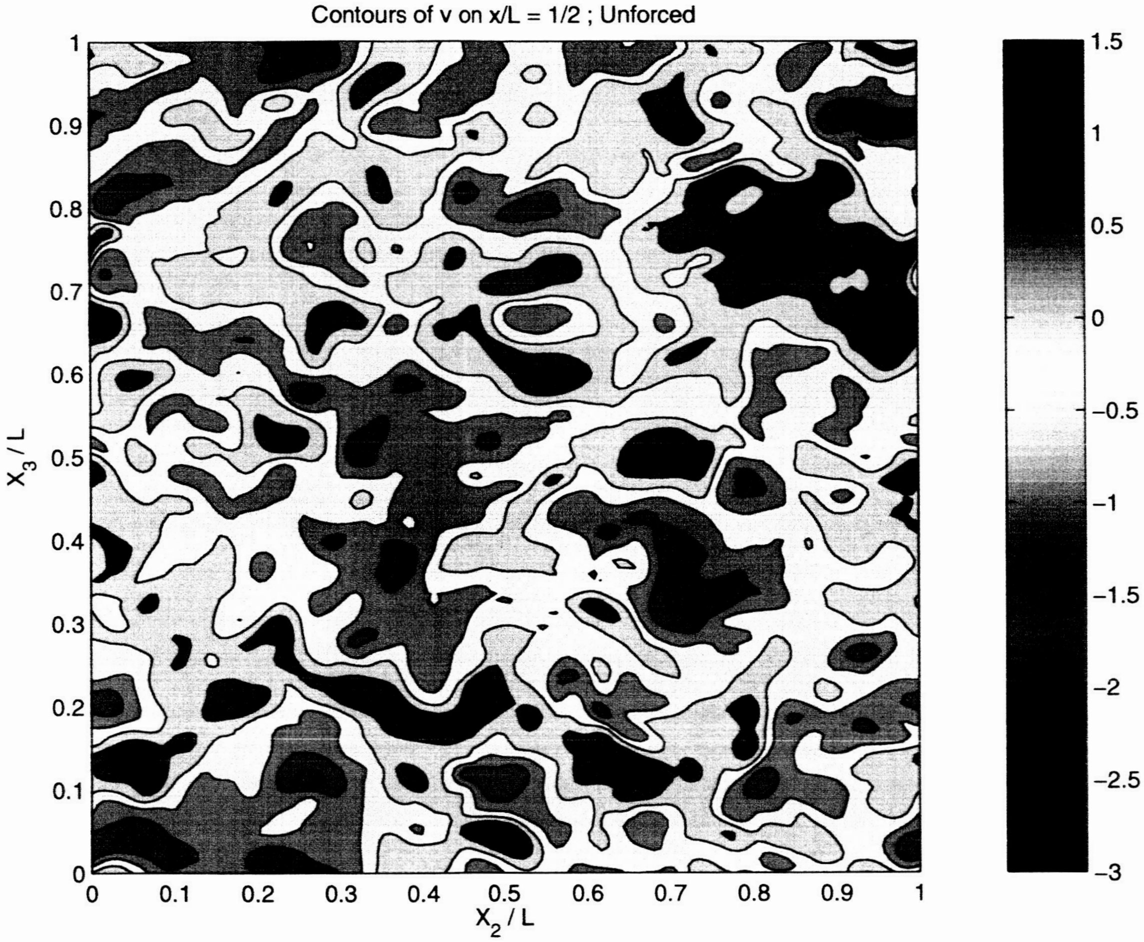

Figure 9: Contours of u_2 on the plane $x_1 = 1/2$ at time t_3 for the unforced flow.

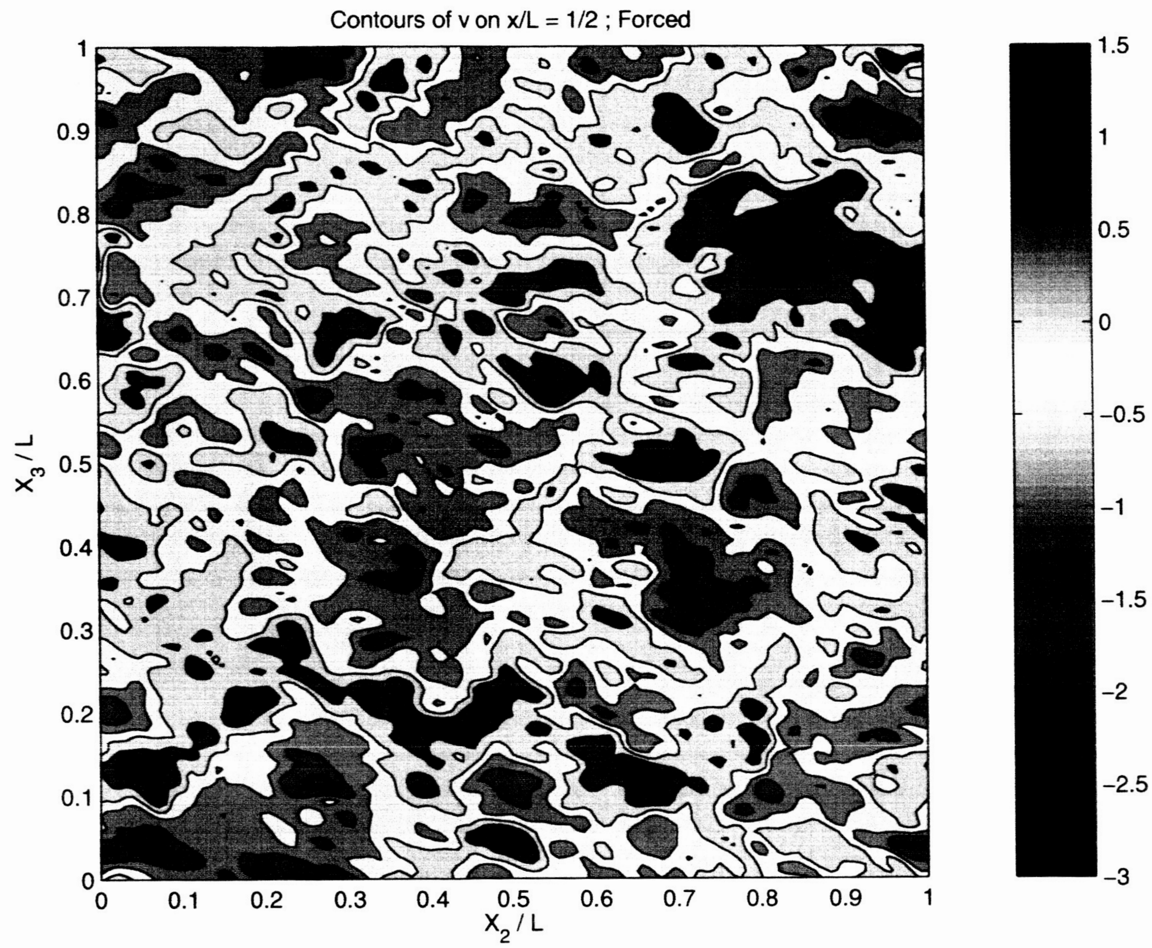

Figure 10: Contours of u_2 on the plane $x_1 = 1/2$ at time t_3 with forcing at high wavenumbers.

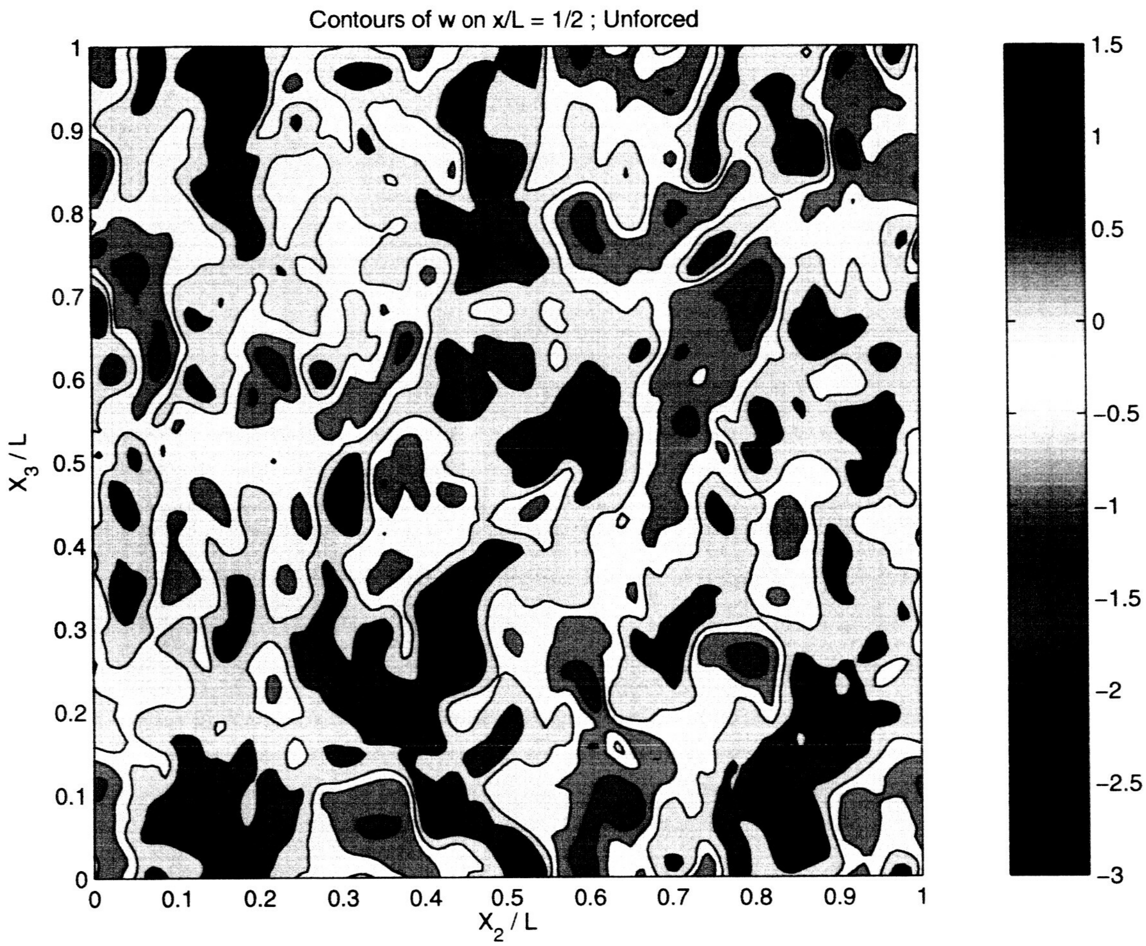

Figure 11: Contours of u_3 on the plane $x_1 = 1/2$ at time t_3 for the unforced flow.

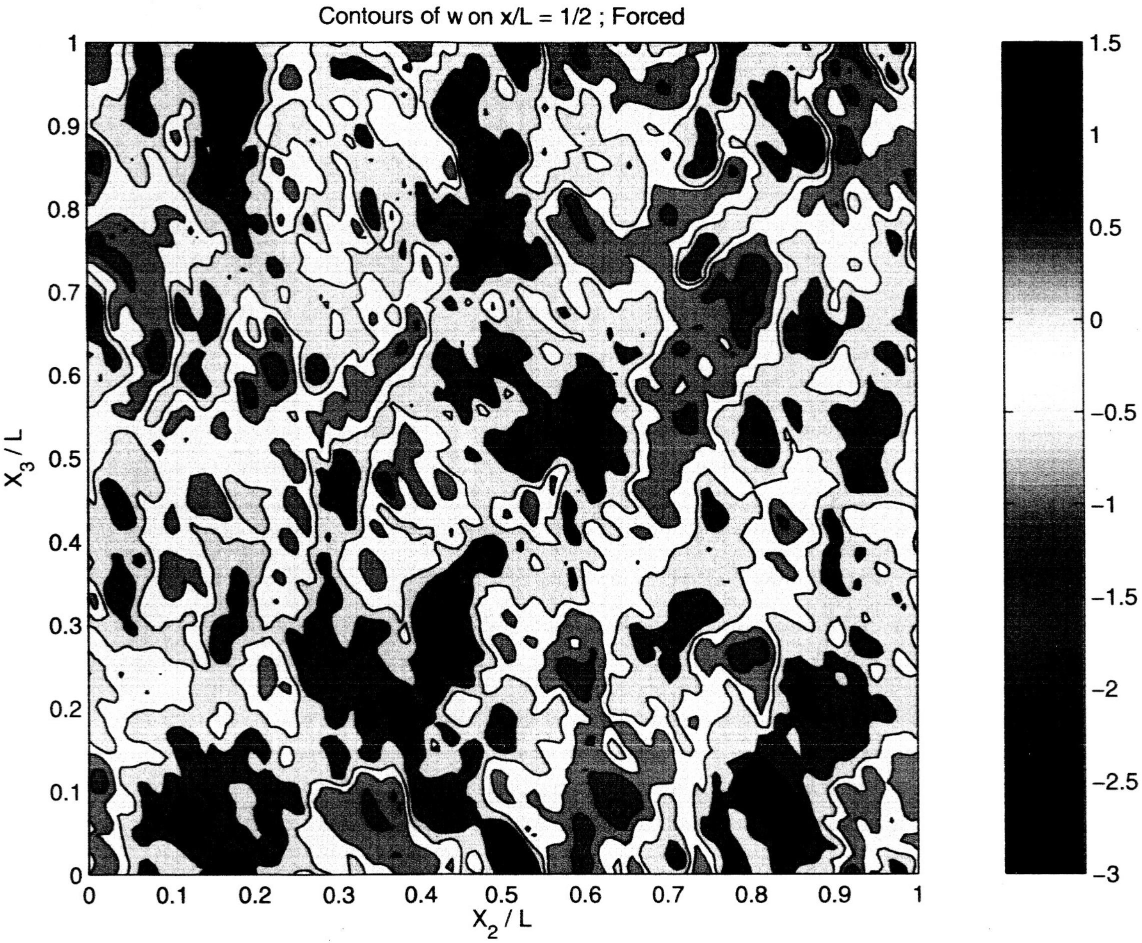

Figure 12: Contours of u_3 on the plane $x_1 = 1/2$ at time t_3 with forcing at high wavenumbers.

Old Dominion University Research Foundation

Document Processing Section
ATTN: Carol Dancy
NASA Center for Aerospace Information (CASI)
7121 Standard Drive
Hanover, MD 21076-1320

RE: Final Report for NASA Research Grant NAG1-1-02005

Dear Carol Dancy:

Enclosed please find a copy of the above referenced report entitled "Studies in Transition and Time Varying Turbulent Flows." The report is being submitted on behalf of Chester E. Grosch, Principal Investigator.
Should you have any questions, or need further assistance, please contact Anna Rogers-Artis at 757-683-4293 ext. 500 or arartis@odu.edu.

Sincerely,

Holland Phillips
Office Services Assistant

Enclosure

P.O. Box 6369 • Norfolk, Virginia 23508-6369
Telephone 757-683-4293 • Facsimile 757-683-5290